

AIRFLOW OVER WAVY YARN IN AIR-JET FILLING INSERTION

Sayavur I. Bakhtiyarov¹ and Sabit Adanur²

¹Space Power Institute, 231 Leach Center, Auburn University, AL 36849-5320

²Textile Engineering Department, Auburn University, AL 36849-5327

ABSTRACT

Airflow over the wavy yarn during air-jet filling insertion is analyzed theoretically. Two flow regimes are considered in the analyses: subsonic and supersonic flows over the yarn. Expression for drag coefficient as a function of air velocity is obtained for both cases. Numerical simulations were made for certain practical situations and comparison is made between the drag force on the yarn in subsonic and supersonic flows.

1. INTRODUCTION

Air-jet weaving is an advanced weaving process where the filling yarn is inserted into the warp shed with a blast of compressed air. An air-jet filling insertion system uses a single nozzle and confusor guide. From the supply package and storage system the yarn is fed into the nozzle through the clamp. The nozzle provides the projection force to the yarn. The confusor guide furnishes orientation to the airflow and yarn. When the insertion is completed, a cutter parts the yarn. To provide high air velocity across the loom, a multi-nozzle system can be used. On this system relay nozzles are used in addition to the main nozzle.

Air-jet weaving process is the most ubiquitously used insertion system in the textile industry. Having very high efficiency and productivity, this system has many advantages over other conventional weaving systems, such as relatively low filling stress on yarn, simple operation, high picking rates, portability, low noise and vibration levels, low cost of spare parts, reduced hazard because of few moving parts, high skilled operators are not required, etc. However this system requires the compressed air which increases the energy costs of the production.

Most theoretical and experimental research efforts are focused on the design of the main nozzle and guide channel to increase efficiency of compressed air.

Uno et al. [1] assumed an exponential decrease of air velocity in the shed of the air-jet loom. They determined that at steady air flow the pressure losses increase with length and cross section changes of the nozzle. Pilipenko [2] reported that the air flow energy in the channel of a pneumatic loom decreases mainly because of kinetic energy losses. The experimental study of air-jet looms with confusor guides [3] showed that the velocity of air jet decreases 4% of its original value at a distance 1.5 m from the nozzle if air is discharged into a free space. When air is discharged from the nozzle to a confusor, the air velocity at a distance of 1.5 m from the nozzle decreases up to 23% of its initial value. The velocity drop depends on the confusor diameter. Using Bernoulli's equation,

Ishida [4] characterized the exit velocity of the air from the nozzle. The effect of the guide tube diameter and configuration on the axial air velocity was studied experimentally in [5-7]. It was found that the pressure increases over the first 30 cm along the guide tube and then decreases. The distance between the guide entrance and nozzle exit has a significant effect on the axial air velocity distribution along the guide tube. The most efficient insertion is achieved when the ratio of tube diameter to nozzle diameter is greater than 1.

A variation of the filling yarn tension during insertion was studied by Kissling [8]. It is shown that the reason for the variation is the super-position of the extremely regular vibration of the yarn in the main jet and the subsequent "flutter" in the free jet beyond the nozzle. Surface properties of the yarn are important factors in filling insertion. Lunenschloss and Wahhoud [9-11] investigated the behavior of yarns in picking with air-jet systems. It is found that insertion time depends on insertion frequency. Authors also reported that yarn velocity in the insertion channel increased with the number of filaments, which increases a contact surface with air. Increased twist on the yarn decreases yarn velocity due to smother surfaces.

Adanur and Bakhtiyarov [12] developed a turbulent-eddy flow model to simulate air flow through the guide channel, which is half open and corrugated. Subsonic air flow in the guide channel was investigated as a simplified model of air flow in a single nozzle air-jet filling insertion system. The drag coefficient in the guide channel and propelling force acting on the yarn were calculated. Numerical simulations of drag coefficient and propelling force were in good agreement with experimental data obtained for the same weaving conditions.

Vangheluwe [13] investigated a rather extended series of bobbins of yarns to determine the influence of yarn properties on the speed of weft insertion in air-jet looms. Author modeled the experimental results using a backpropagation neural network, giving a correlation coefficient of 0.97183 between the experimental and calculated loom angles at weft arrival. Author studied the influence of yarn count, diameter, hairiness, evenness, and their interactions on the weft arrival angle using the neural network model.

The geometric structure of the yarn is completely irregular and flexible, which complicates the analysis of yarn motion. In this paper we present the results of the theoretical analyses of air flow over the wavy yarn during air-jet filling insertion. Two flow regimes are considered in these analyses: subsonic and supersonic flows over the yarn. Expression for drag coefficient as a function of air velocity is obtained for both cases. Numerical simulations were made for certain practical situations and comparison is made between the drag force on the yarn in subsonic and supersonic flows.

2. THEORETICAL ANALYSES

The motion of the filling yarn in air-jet insertion is provided by compressed air. A yarn cannot simply be represented by a right cylinder [13]. Airflow can be considered as sequence of compressible and incompressible flows due to instabilities and turbulence. Therefore the yarn in the airflow field has inflections in axial direction. These inflections may have significant impact on the yarn filling performances and compressed air efficiency. In the first approach the inflected yarn may be considered as a wave-shaped cylinder.

2.1. Subsonic air flow over a wavy yarn

Consider a uniform subsonic airflow in the horizontal (x) direction. Assume the airflow passes over a wave-shaped cylindrical yarn with velocity U_{air} (Figure 1). The yarn walls can be described by the equation:

$$\xi = A \sin \frac{2\pi\psi}{\lambda}, \quad (1)$$

where $\psi = \frac{x}{D}$, $\xi = \frac{y}{D}$, $A = \frac{A_{yarn}}{D}$, $\lambda = \frac{\lambda_{yarn}}{D}$, D is a diameter of yarn, A_{yarn} is an amplitude of the yarn surface waves, λ_{yarn} is a period of waves. In practical situations A is much less than λ . Therefore small perturbation theory can be applied in this case.

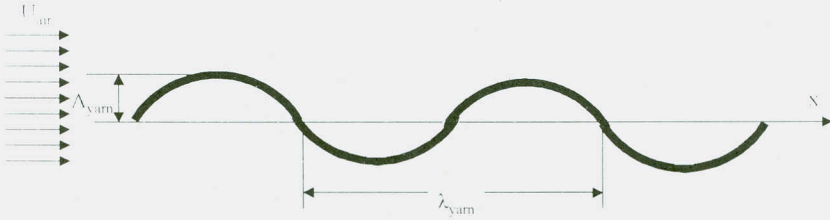


Figure 1. Schematics of airflow over wavy cylindrical yarn.

Then the problem will reduce to the following partial differential equation:

$$(1-M^2) \frac{\partial^2 \varphi}{\partial \psi^2} + \frac{\partial^2 \varphi}{\partial \xi^2} = 0, \quad (2)$$

with the boundary conditions:

$$v(\psi_w, 0) = U_{air} \left(\frac{d\xi}{d\psi} \right)_w = \bar{U} A \frac{2\pi}{\lambda} \cos \frac{2\pi\psi}{\lambda}, \quad (3)$$

where φ is a velocity potential defined as a function of the space coordinates and time; M is a Mach number; $\bar{U} = U_{air} - U_{yarn} - \Delta u$, U_{air} is an average air velocity, U_{yarn} is a velocity of yarn, Δu is velocity losses due to friction forces on yarn surface.

To solve the linear partial differential equation (2) we assume that the potential function φ is a product of functions Ψ and Ξ , where Ψ is a function of ψ alone, and Ξ is a function of ξ alone. Then,

$$\varphi = \Psi(\psi) \Xi(\xi). \quad (4)$$

Substituting (4) into equation (2) gives:

$$\frac{1}{\Psi} \frac{d^2 \Psi}{d\psi^2} = - \frac{1}{(1-M^2)\Xi} \frac{d^2 \Xi}{d\xi^2} \quad (5)$$

Since the left-hand side of equation (5) is dependent on ψ alone, and the right-hand side is dependent on ξ , we can write:

$$\frac{d^2 \Psi}{d^2 \psi} + \sigma^2 \Psi = 0, \quad (6)$$

$$\frac{d^2 \Xi}{d\xi^2} - (1-M^2)\sigma^2 \Xi = 0. \quad (7)$$

The solutions of these two ordinary differential equations are:

$$\Psi = C_1 \cos \sigma \psi + C_2 \sin \sigma \psi, \quad (8)$$

$$\Xi = C_3 \exp\left[\left(\sqrt{1-M^2}\right)\sigma\xi\right] + C_4 \exp\left[-\left(\sqrt{1-M^2}\right)\sigma\xi\right] \quad (9)$$

From the boundary conditions at the wall ($\xi=0$):

$$v = -\frac{\partial \varphi}{\partial \xi} = \bar{U} A \frac{2\pi}{\lambda} \cos \frac{2\pi\psi}{\lambda} \quad (10)$$

we determine the constants as following:

$$C_2 = C_3 = 0, \quad C_1 C_4 = \frac{\bar{U} A}{\sqrt{1-M^2}} \quad (11)$$

Finally we obtain an expression for potential function:

$$\varphi = \frac{\bar{U} A}{\sqrt{1-M^2}} \exp\left[-\left(1-M^2\right)\left(\frac{2\pi}{\lambda}\right)\xi\right] \cos \frac{2\pi\psi}{\lambda} \quad (12)$$

The nondimensional pressure coefficient C_p for subsonic airflow over the wavy yarn will be determined as:

$$C_p = \frac{p - p_\infty}{\frac{1}{2} \rho \bar{U}^2} = - \frac{4\pi A}{\lambda \sqrt{1-M^2}} \sin \frac{2\pi\psi}{\lambda} \quad (13)$$

2.1. Supersonic air flow over a wavy yarn

For supersonic flows in which $M > 1$, the coefficient of the first term in equation (2) becomes negative. For $M < 1$ an elliptic type partial equation was reduced to Laplace's equation. However, for $M > 1$ equation (2) is of the hyperbolic type. For our problem the potential function can be written as:

$$\phi = \zeta \left(\psi' - \xi \sqrt{M^2 - 1} \right) \quad (14)$$

where ζ is an arbitrary function

The boundary conditions at the yarn walls will be the same as for the subsonic airflow case. Substituting equation (14) into equation (3) we obtain expression for the potential function, and then for the pressure coefficient over a wave-shaped yarn:

$$C_p = \frac{4\pi A}{\lambda \sqrt{M^2 - 1}} \cos \frac{2\pi \psi'}{\lambda} \quad (15)$$

3. RESULTS AND DISCUSSION

The results of calculation for the airflow streamlines along the yarn walls for subsonic flow is presented in Figure 2. As seen from the figure, the flow disturbances created by the yarn decreases with distance from the yarn surface. Figure 3 shows a variation of the amplitudes of the disturbances with distance from the yarn surface at different air velocities. As shown in this figure, the amplitude of disturbances decreases with both air velocity and distance from the yarn.

Variation of velocity potential per function ζ along the yarn for supersonic flow is presented in Figure 4. As seen from the figure, the ratio ϕ/ζ increases along the yarn, but it decreases with distance from the yarn surface.

Variation of the calculated pressure coefficients for subsonic ($M=0.1$) and supersonic ($M=1.1$) airflow along the yarn walls is presented in Figure 5. As we expected, the pressure coefficient values at supersonic flow are significantly higher than pressure coefficients for subsonic flows.

4. CONCLUSIONS

Theoretical analyses are conducted for airflow over the wavy yarn during air-jet filling insertion. Two flow regimes are considered in the analyses, subsonic and supersonic flows over the yarn. Expression for drag coefficient as a function of air velocity is obtained for both cases. Numerical simulations show substantial difference of both velocity potentials and pressure distributions along the yarn walls at subsonic and supersonic airflow regimes.

REFERENCES

1. M. Uno, A. Shimomi and H. Kise, A Study of an Air-Jet Loom with Substreams Added, Part 2: Analysis of Various Weaving Factors by the Equation of Motion of Weft, *J. Textile Mach. Soc. Japan*, 18 (3), 86-92, 1972.

2. V. A. Pilipenko, Analysis of the Air Flow in the Channel of Pneumatic Looms, *Tech. Textile Ind. USSR*, 3, 137-142, 1965.
3. V. Horn, New Range of Jettis Air-Jet Looms, *Investa*, 1, 1976.
4. T. Ishida, Air-Jet Loom, Present and Future, Part 3: How Air-Jet Expands in the Shed, *Int. Textile Mag.*, 8 (336), 83-85, 1982.
5. M. M. Salama, Mechanics of Air-Jet Filling Insertion, Ph.D. Thesis, North Carolina State University, 1984.
6. M. H. Mohamed and M. Salama, Mechanics of a Single Nozzle Air-Jet Filling Insertion System, Part I: Nozzle Design and Performance, *Textile Research Journal*, 56 (11), 683-690, 1986.
7. M. Salama and M. H. Mohamed, Mechanics of a Single Nozzle Air-Jet Filling Insertion System, Part II: Velocity Distribution and Design of the Air Guide System, *Textile Research Journal*, 56 (12), 721-726, 1986.
8. U. Kissling, Measuring Rig for Investigating Weft Insertion on Air-Jet Looms, *Textile Prac. Int.*, 8, ii-iv, 1983.
9. J. Lunenschloss and A. Wahhoud, Weft Insertion Behavior of Yarns During Air-Jet Weaving by Jet and Drum Store, *Chemiefasern / Textilind.*, 4, 266-268, 1983.
10. J. Lunenschloss and A. Wahhoud, Investigation into the Behavior of Yarns in Picking with Air-Jet Systems, *Melliand Textilber. Eng. Ed.*, 4, 228-231, 1984.
11. J. Lunenschloss and A. Wahhoud, Picking Behavior of Continuous Filament Yarns in Air-Jet Weaving, *Melliand Textilber. Eng. Ed.*, 5, 288-292, 1984.
12. S. Adanur and S. I. Bakhtiyarov, Analysis of Air Flow in Single Nozzle Air-Jet Filling Insertion: Corrugated Channel Model, *Textile Research Journal*, 66 (6), 401-406, 1996.
13. L. Vangheluwe, Weft Insertion of Polyester/Cotton Blend Yarns on Air-Jet Looms, *Textile Research Journal*, 67 (11), 809-815, 1997.

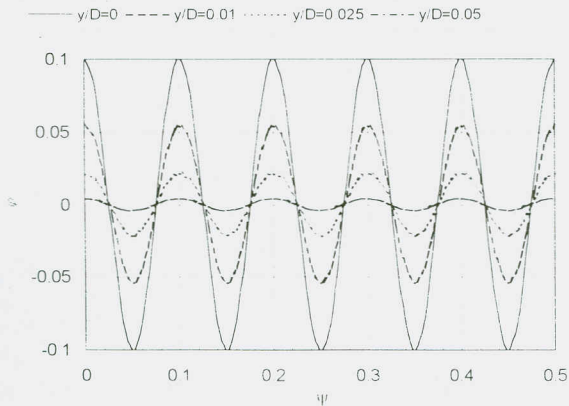


Figure 2. Airflow streamlines in the vicinity of the yarn for subsonic flow ($\bar{U} = 100$ m/s, $A=0.001$, $M=0.1$, $\lambda=0.1$).

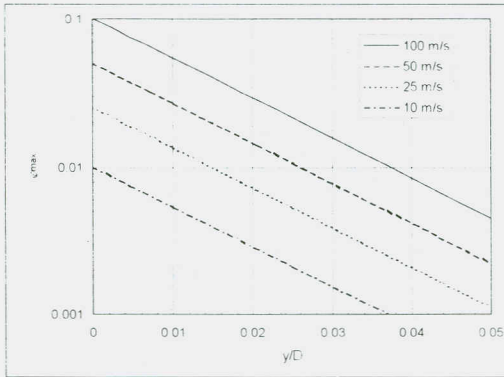


Figure 3. Variation of the amplitudes of disturbances with distance from the yarn surface at different air velocities ($\nu = 0.1$, $A = 0.001$, $M = 0.1$, $\lambda = 0.1$).

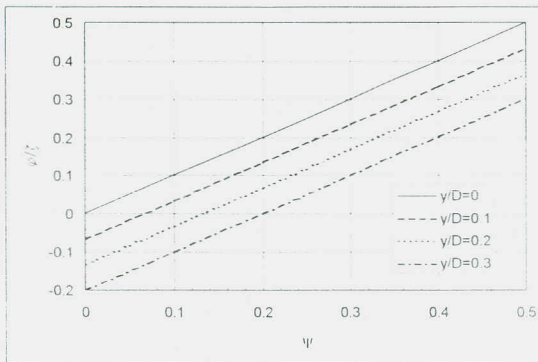


Figure 4. Airflow streamlines in the vicinity of the yarn for supersonic flow ($M = 1.2$).

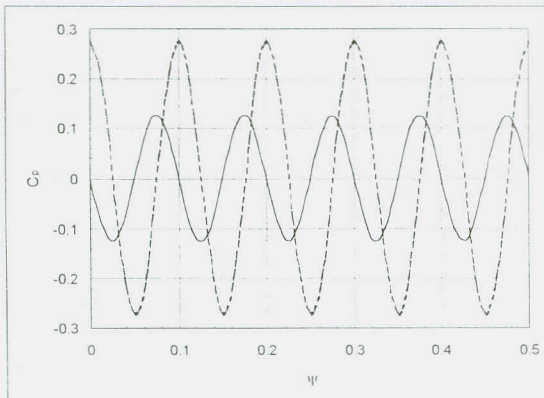


Figure 5. Variation of pressure coefficient for subsonic (— $M = 0.1$) and supersonic (---- $M = 1.1$) airflow over the wavy yarn.